

Stoichiometry, Thermal Stability and Reducibility of Perovskite-Type Mixed Oxide LaBO_3 (B = Fe, Co, Ni)

Il-Hyun Park* and Hyung-Pyo Lee

Department of Chemistry, Sung Kyun Kwan University, Natural Science Campus, Suwon 440-746

Received March 29, 1988

The titled properties on reduction of the perovskite LaBO_3 (B = Fe, Co, Ni) have been investigated by means of temperature-programmed reduction, isothermal reduction and X-ray diffraction methods. Nominal composition of $\text{LaFeO}_{3.18}$, $\text{LaCoO}_{3.00}$ and $\text{LaNiO}_{2.92}$ are determined. Reduction reaction of these mixed oxides differed according to B-site transition metal and thermal stability on reduction decreased as following order: $\text{LaFeO}_{3.18} > \text{LaCoO}_{3.00} > \text{LaNiO}_{2.92}$. From the results of isothermal reaction, kinetics on reduction of the perovskite has been discussed in detail.

Introduction

LaBO_3 perovskite, where B being transition metal, with general formula of ABO_3 has been extensively studied in the field of solid state chemistry and catalysis. Over the last few decades, as rival material of noble metal for automotive exhaust catalyst, lanthanum transition metal oxides are of considerable interest because of their promising applicability for redox catalyst.^{1,4} George and Viswanathan⁵ studied the oxidation kinetics of CO on LnCoO_3 (Ln = La, Nd, Sm or Gd), and Tascon *et al.*⁶ assumed the rate controlling step of CO oxidation to be the surface reaction between adsorbed CO and dissociatively adsorbed O_2 . Petunchi *et al.*⁷ found that LaCoO_3 is active for hydrogenation of ethylene when the perovskite is in the reduced state at 300-490 °C, afterward the nature of active sites on reduction was investigated by means of X-ray photoelectron spectroscopy.⁸ Ichimura *et al.*⁹ also examined the hydrogenolysis of ethene and ethane or C_3 - C_5 alkanes on LaCoO_3 . Arakawa *et al.*¹⁰ made search on the crystallographic properties of rare earth cobaltate perovskite during reduction under high pressure of H_2 using the X-ray diffraction and thermogravimetric analysis. On the other hand, LaNiO_3 is similar in surface properties to LaCoO_3 and thus shows analogous redox behaviors. Hydrogenation of ethylene on reduced LaNiO_3 was studied by Crespin *et al.*¹¹ LaFeO_3 has relatively lower catalytic activity than the other perovskites but it has been reported that partial substitution of Sr^{2+} ion on A site (La) causes the activity to increase at low content of dopant (Sr^{2+}).¹² Tascon *et al.*¹³ investigated the kinetic behaviors on reduction and oxygen adsorption of LaFeO_3 with the use of a gravimetric measurement. Electronic properties and defect structure of LaFeO_3 and Sr-doped LaFeO_3 have been reported by Misusaki *et al.*¹⁴

It has been well known that physicochemical properties of the perovskite vary with the electronic state of transition metal ion¹⁵, and preparation method is also responsible for the valence state of transition metal regarding to oxygen stoichiometry, stability and reactivity.¹⁶ In general, non-stoichiometric structure of the perovskite is caused due to the vacancy of A and/or B cation which affects considerably both surface and bulk properties.¹⁵ Thus, characterization of the perovskite prior to the testing of reactivity and consideration of relationships between available parameters are primarily important.

In the present work, oxygen stoichiometry and reducibility of lanthanum iron and cobalt oxides prepared by cyanide

decomposition and lanthanum nickel oxide by conventional ceramic method have been examined. In addition, detailed informations including reaction mechanism and kinetics on reduction of these perovskites have been described.

Experimental

Material. Perovskite-type lanthanum iron and cobalt oxides¹⁷ were prepared by thermal decomposition in air (650 °C, 6h) of cyano complex precipitated from lanthanum nitrate (Fluka AG Grade) and potassium iron(cobalt) cyanide (BDH, 99% minimum purity). Lanthanum nickel oxide¹⁸ was obtained by solid state reaction (850 °C, 36h) in air of lanthanum (Aldrich, 99.9%) and nickel (Aldrich, 99.99%) oxides with sodium carbonate flux. The X-ray diffraction patterns of the sample perovskite showed no peaks corresponding to the secondary phase (Fig. 2-a, c,e). H_2 gas (99.99%, Matheson, USA) used in this work was purified through cold trap at liquid nitrogen temperature.

Methods. Reduction processes of the perovskite LaBO_3 (B = Fe, Co, Ni) have been studied by means of temperature-programmed reduction (TPR) method. TPR experiment has been carried out using a sensitive quartz spring balance in the home-made glass vacuum apparatus.¹⁹ Weight change of the sample through the reaction was detected by a cathetometer having a maximum sensitivity of 5×10^{-3} mm, and thus every TPR runs are preserved about 10^{-5} g accuracy. The extent of reduction was measured directly from the weight decrease of the sample. About 80 mg sample was loaded in a quartz basket (ca. 170 mg, 0.2 ml) and the system was maintained under 10^{-6} torr atmosphere for 2h at room temperature. After this pretreatment, 300 torr H_2 was admitted to the system and the sample was reduced at 5 °C per min heating rate using a programmed temperature controller. Reduction temperature of the sample was measured by a Pt/Pt-Rh (10%) thermocouple positioned near the sample basket. Water vapor formed during reduction was swept from the reaction zone using a liquid nitrogen cold trap. For the isothermal reduction study, temperature was elevated to the desired reduction one and then the system was maintained in dynamic vacuum of 10^{-5} torr. Afterward, H_2 gas (300 torr) was introduced into the system. Weight change of the sample at fixed reduction temperature was measured at one minute interval. Fresh sample oxide was used in each kinetic study.

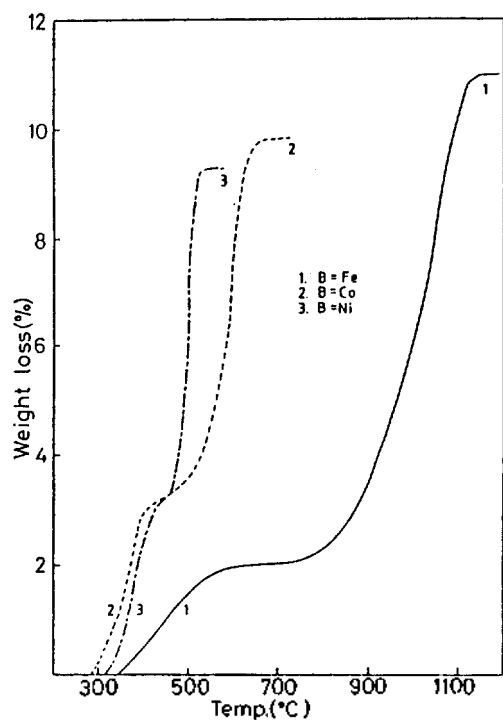


Figure 1. Temperature-programmed reduction profiles of the perovskite $\text{LaBO}_{3\pm y}$ in 300 torr H_2 at heating rate of 5 °C per min.

X-ray phase analysis of the sample powder has been performed by the use of a Rigaku-Denki diffractometer (Geigerflex, D/Max-III B) with Ni-filtered $\text{CuK}\alpha$ radiation.

Results and Discussion

Oxygen stoichiometry. The results of temperature-programmed reduction of $\text{LaBO}_3(\text{B} = \text{Fe}, \text{Co}, \text{Ni})$ oxide are given in Figure 1. It shows that reducibilities exhibit the different characteristics according to the transition metal site (B-site) in the perovskite. Powder X-ray diffraction patterns, as shown in Figure 2(b,d,f), of the final reduction products obtained from each perovskite show only lanthanum (III) oxide and the corresponding metal phase. This fact indicates that all the perovskite samples are completely changed to La_2O_3 and metals regardless of transition metal ion. On the other hand, total weight loss of lanthanum iron, cobalt and nickel oxide are 11.1, 9.75 and 9.27%, respectively. Considering the stoichiometric composition, it has shown that lanthanum iron oxide was reduced more than the theoretical amount but lanthanum nickel oxide slightly less than the theoretical one. For the reduction of lanthanum cobalt oxide, the degree of reduction up to the final stage is nearly equivalent to the theoretical amount. These results directly imply that lanthanum iron and nickel oxide samples have the non-stoichiometric composition while lanthanum cobalt oxide results in the stoichiometry.

The degree of deviation from stoichiometry in the perovskite sample is calculated from the following relationship: $y(\text{in } \text{LaBO}_{3\pm y}) = W_O(\Delta W_m - \Delta W_C)/W_S$, where W_S is initial sample weight, ΔW_m total weight loss of the sample after reduction, ΔW_C calculated weight loss corresponding to 3 e^- per molecule reduction, $\text{LaBO}_3 + 1.5\text{H}_2 \rightarrow 0.5\text{La}_2\text{O}_3 + \text{B}^0 + 1.5\text{H}_2\text{O}$, and W_O atomic weight of oxygen. Oxygen stoichiometry determined from above equation for lanthanum iron, co-

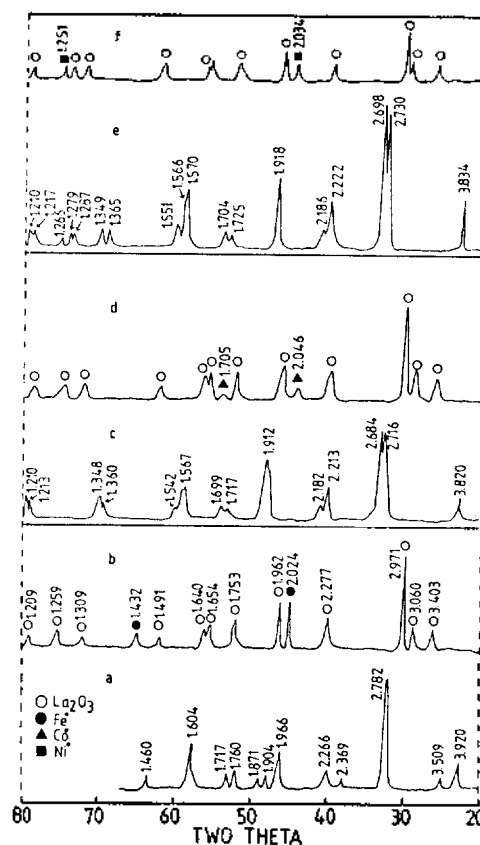


Figure 2. X-ray diffraction patterns of the perovskites and their reduction products. (a): Lanthanum iron oxide, (b): Reduced phase of sample (a) at 1130 °C, (c): Lanthanum cobalt oxide, (d): Reduced phase of sample (c) at 655 °C, (e): Lanthanum nickel oxide, (f): Reduced phase of sample (e) at 530 °C.

balt and nickel oxide is $\text{LaFeO}_{3.18}$, $\text{LaCoO}_{3.00}$ and $\text{LaNiO}_{2.92}$, respectively. Oxygen-deficient nickel perovskite is expected due to the preferential stability of divalent Ni, and lanthanum iron oxide usually shown non-stoichiometry with excess oxygen in the perovskite.¹⁵ And, some lanthanum cobalt oxides exhibit the oxygen-deficient structure¹⁵ but stoichiometric composition obtained in this work is probably resulted from the lower preparation temperature (650 °C). When the perovskite is in the non-stoichiometry, the charge balance could be attained by self-redox of transition metal ion formulating by $\text{La}^{3+}\text{B}_{1-2y}^{3+}\text{B}_{2y}^{4+}\text{O}_{3+y}$ or $\text{La}^{3+}\text{B}_{1-2y}^{3+}\text{B}_{2y}^{2+}\text{O}_{3-y}$. It is therefore appropriate to assume that lanthanum iron oxide used in this work contains Fe^{4+} ion of about 36% and lanthanum nickel oxide does Ni^{2+} ion of about 16% as impurity to balance the oxygen stoichiometry. This fact was also observed in $\text{SrCoO}_{2.5}$ ²⁰ and $\text{La}_{1-x}\text{Sr}_x\text{CoO}_3$.²¹ In addition, it has been confirmed in this laboratory²² that lanthanum manganese oxide prepared by the coprecipitation method shows the oxidative non-stoichiometry with chemical composition of $\text{LaMnO}_{3.15}$.

It has been well established that lanthanum transition metal oxide gives the wide range in oxygen stoichiometry according to the preparative condition and that, in general, when the perovskite is prepared at higher temperature, the content of oxygen decreases.¹⁵ The non-stoichiometry in both lanthanum iron and nickel oxides has been also observed by several workers. Wachowski *et al.*²³ found the non-stoi-

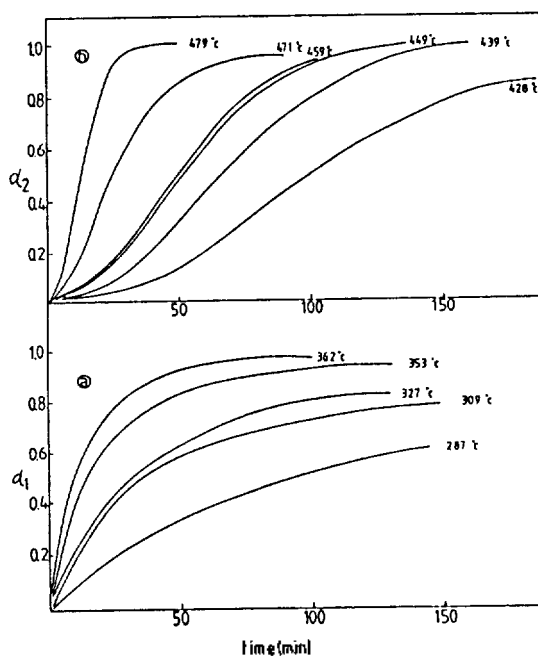
Table 1. Reducibilities of the Perovskite $\text{LaBO}_3\text{B} = \text{Fe, Co, Ni}$ in 300 torr H_2 at Heating Rate of 5 °C per min.

	$\text{LaFeO}_{3.18}$			$\text{LaCoO}_{3.00}$			$\text{LaNiO}_{2.92}$		
	Reduction temp. interval (°C)	Extent of reduction %	e^-	Reduction temp. interval (°C)	Extent of reduction %	e^-	Reduction temp. interval (°C)	Extent of reduction %	e^-
1st stage	$\text{LaFeO}_{3.18} + 0.18\text{H}_2 \longrightarrow \text{LaFeO}_3 + 0.18\text{H}_2\text{O}$			$\text{LaCoO}_3 + 0.5\text{H}_2 \longrightarrow \text{LaCoO}_{2.5} + 0.5\text{H}_2\text{O}$			$\text{LaNiO}_{2.92} + 0.42\text{H}_2 \longrightarrow \text{LaNiO}_{2.5} + 0.42\text{H}_2\text{O}$		
	300-550	1.8	-	285-415	3.3	1.01	330-445	3.24	0.99
2nd stage	$\text{LaFeO}_3 + 1.5\text{H}_2 \longrightarrow 0.5\text{La}_2\text{O}_3 + \text{Fe} + 1.5\text{H}_2\text{O}$			$\text{LaCoO}_{2.5} + \text{H}_2 \longrightarrow 0.5\text{La}_2\text{O}_3 + \text{Co} + \text{H}_2\text{O}$			$\text{LaNiO}_{2.5} + \text{H}_2 \longrightarrow 0.5\text{La}_2\text{O}_3 + \text{Ni} + \text{H}_2\text{O}$		
	800-1130	11.1	3.0	460-655	9.75	3.0	455-530	9.27	2.85

chometric compounds of $\text{LaFeO}_{3.22}$ and $\text{LaNiO}_{2.98}$ as the sample perovskites are prepared applying the explosion method in air stream. Taking into account the lower calcination temperature (500 °C) adopted by these authors, slightly higher content of oxygen than the present results in both perovskites could be readily understood. However, the report by Tascon *et al.*¹³ showed same non-stoichiometry in lanthanum iron oxide as that observed by the present authors.

Reduction reaction and stability. As confirmed in Figure 1, reducibilities of lanthanum cobalt and nickel oxides gave similar characteristics but lanthanum iron oxide showed different behavior. The temperature-programmed reduction of the former perovskites exhibited two distinct plateaus with the formation of reduction levels of 1 and 3 electrons while the latter was directly reduced through a horizontal level corresponding to about 1.8% weight loss to final products. It means that lanthanum cobalt and nickel oxides are reduced to La_2O_3 and metallic Co or Ni (Fig. 2) *via* the intermediate having chemical composition of $\text{LaCoO}_{2.5}$ or $\text{LaNiO}_{2.5}$ and that non-stoichiometric lanthanum iron oxide is first reduced to stoichiometric compound and finally to La_2O_3 and Fe^0 . It is also concluded that the first reduction product having the stoichiometric composition is comparatively stable because the phase exists in the wide temperature range (550-800 °C). And, it is assumed that in the first reduction stage of non-stoichiometric iron perovskite the impurity of iron(IV) cation existed in the perovskite converted into lower oxidation state Fe^{3+} . Similar results have been discussed by Wachowski *et al.*²³ and Tascon *et al.*¹³ In addition, Wachowski *et al.*²³ found that stoichiometric lanthanum iron oxide was reduced in a flow of 10% H_2 and 90% N_2 to the oxidation state of Fe^{2+} corresponding to the reduction level of 2 electrons prior to 3-electron reduction. For reference, according to the results obtained in this laboratory²², it was verified that the oxidative lanthanum manganese oxide, $\text{LaMnO}_{3.15}$, was reduced through stoichiometric compound to lanthanum(III) and manganese(II) oxides, corresponding to 1-electron reduction, as final products.

The TPR results of the perovskite used in this work are summarized in Table 1 including reduction processes. It clearly shows that although lanthanum nickel oxide began to reduce at higher temperature (330 °C) than lanthanum cobalt oxide (285 °C), the former was leveled off at much lower temperature (530 °C) than the latter (655 °C). On the other hand, lanthanum iron oxide has the highest reduction temperature among these perovskites, indicating the highest stability. This is similar to the result confirmed by Wachowski *et al.*²³ with the exception of reduction temperature


Figure 3. Reduction isotherms of $\text{LaNiO}_{2.92}$ at lower (a) and higher (b) temperature regions.

and, for reference, they compared the thermal stability on reduction of the perovskite with simple oxide Fe_2O_3 , Co_3O_4 and NiO. It was also observed in this laboratory²² that lanthanum manganese oxide, one of a series of lanthanum transition metal oxide, is less stable than lanthanum iron oxide but more stable than lanthanum cobalt and nickel oxides. Nakamura *et al.*²⁴ has reported the same conclusion as that found by the present authors.

Reduction kinetics. Kinetic studies on reduction of $\text{LaBO}_3\text{B} = \text{Fe, Co, Ni}$ oxide are carried out at each reduction stage (Table 1). Figure 3, 4 and 5-a give kinetic curves for the reduction of lanthanum nickel, cobalt and iron oxides, respectively. In the case of non-stoichiometric lanthanum iron oxide, only reduction process of stoichiometric compound corresponding to 3-electron reduction is considered for the reason of less reproducibility of kinetic data obtained in the first reduction stage. Tascon *et al.*¹³ explained this reaction stage below 727 °C as very slow reduction process. Nevertheless, present authors will discuss on this fact in the other study.

The degree of reduction, α_i , was calculated by the relationship: $\alpha_i = \Delta W_t / \Delta W_m$, where ΔW_t is weight loss of the oxide sample after time t and ΔW_m maximum loss in weight

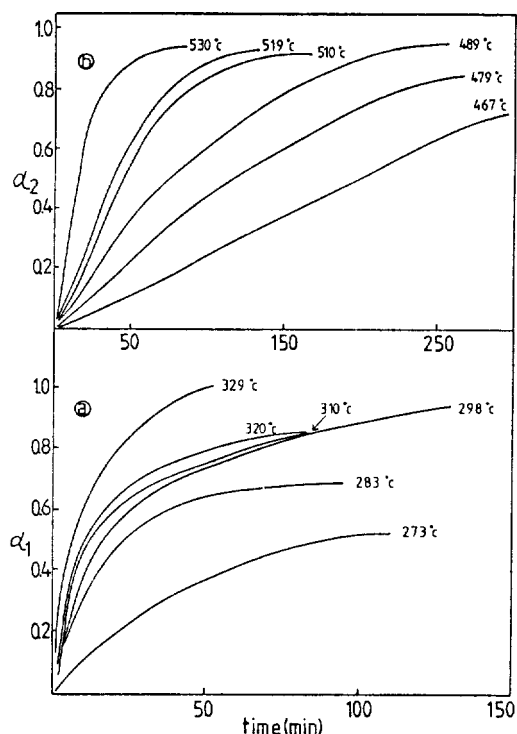


Figure 4. Reduction isotherms of LaCoO_3 at lower(a) and higher(b) temperature regions.

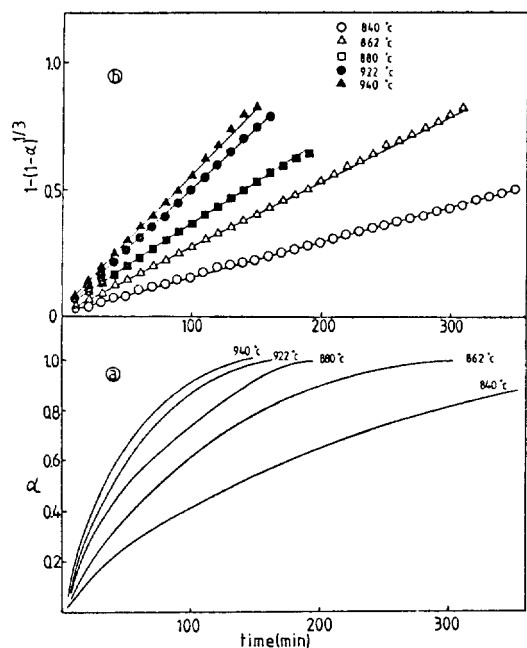


Figure 5. (a) Reduction isotherms of LaFeO_3 . (b) Linear plots of $1-(1-\alpha)^{1/3}$ vs t for the reduction of LaFeO_3 .

of the sample for each reduction stage (Table 1). The kinetic curves are analyzed in the following procedures: Each set of data (α, t) is calculated using a conventional least square method to fit with the rate equations and reduction models collected in Table 2. The calculation is performed by the use of a personal computer and minimum standard deviation (σ) is used to select the optimum reduction model, and activation energy (E_a) and preexponential coefficient (A) are calculated using Arrhenius equation from the corresponding data set

Table 2. Rate Equations and Models in Reduction Kinetic Studies

Rate controlling mechanism	Reduction model	Equation, $f(\alpha)$
Diffusion of reactant through the reacted zone	One dimensional diffusion	$\alpha^2 = k_1 t$
	Two dimensional diffusion	$(1-\alpha)\ln(1-\alpha) + \alpha = k_2 t$
	Three dimensional diffusion according to Jander	$[1-(1-\alpha)^{1/3}]^2 = k_3 t$
	Three dimensional diffusion according to Ginstling-Brounshtein	$1-(2\alpha/3)-(1-\alpha)^{2/3} = k_4 t$
Chemical reaction at phase boundary	Contracting cylinder	$1-(1-\alpha)^{1/2} = k_5 t$
	Contracting sphere	$1-(1-\alpha)^{1/3} = k_6 t$
Nuclei formation	Avrami-Erofeev	$[-\ln(1-\alpha)]^{1/2} = k_7 t$
		$[-\ln(1-\alpha)]^{1/3} = k_8 t$

(T.k).²²

Numerical data on reduction of the perovskite, including kinetic parameters, are summarized in Table 3. It apparently shows that the first and second reduction stage in both lanthanum nickel and cobalt oxides are followed by Ginstling-Brounshtein model ($\sigma = 0.8\%$ for lanthanum nickel oxide; $\sigma = 0.76\%$ for lanthanum cobalt oxide) and Avrami-Erofeev model ($\sigma = 2.1\%$, $n = 3$ for lanthanum nickel oxide; $\sigma = 2.2\%$, $n = 2$ for lanthanum cobalt oxide), respectively, while reduction kinetics of lanthanum iron oxide is controlled by contracting sphere model ($\sigma = 1.24\%$). From these results, it can be inferred that 1-electron reduction of lanthanum nickel and cobalt oxides is governed by three dimensional diffusion of reactant through the reacted zone.²⁵ Namely, in consequence of rapid nucleation on the surface of metal oxide very soon after initiation of reaction, thin layers of product nuclei are completely covered over all the reactant oxide surface and then the reaction interface between reactant and product advances inward as reaction progresses. The rate process followed by diffusion mechanism is therefore deceleratory throughout the reaction. This type of kinetic behavior has been discussed by Arnoldy *et al.*²⁶ who presented that reduction reaction of MoO_3 to MoO_2 by H_2 is controlled by oxygen diffusion mechanism following very fast elimination of oxygen atoms at the oxide surface.

Reaction in the second reduction stage of lanthanum nickel and cobalt oxides, as shown in Table 3, is controlled by nuclei formation and growth mechanism.²⁷ At initial reaction duration, the product nuclei are randomly formed at the specific potential sites with the eventual elimination of oxygen ions from the oxide lattice and then slowly grew. The reaction interface begins to increase more rapidly until growing nuclei overlap mutually. As the metal oxide is consumed by overlapping of nuclei, the rate of reduction decreases continuously, resulting the sigmoid in shape of reduction isotherms (Figure 3-b, 4-b). The sigmoidal kinetic characteristics has been confirmed in many metal oxide systems such as CuO , Co_3O_4 ²⁷ and NiO .²⁸ Recently, Fierro *et al.*²⁹ reported that the second reduction stage of lanthanum nickel oxide exhibited the nucleation mechanism, as confirmed in the present study. In addition, it has shown in this laboratory²² that reduction kinetics of LaMnO_3 is followed by nucleation mechanism.

On the other hand, reduction rate of lanthanum iron oxide

Table 3. Evaluation of Kinetic Data on Reduction of the Perovskite LaBO_3 (B = Fe, Co, Ni)

Reduction equation	LaFeO_3			LaCoO_3			$\text{LaNiO}_{2.92}$		
	E_a (Kcal/mole ⁻¹)	Preexp.term $\ln A(\text{sec}^{-1})$	Av.st.dev. (%)	E_a (Kcal/mole ⁻¹)	Preexp.term $\ln A(\text{sec}^{-1})$	Av.st.dev. (%)	E_a (Kcal/mole ⁻¹)	Preexp.term $\ln A(\text{sec}^{-1})$	Av.st.dev. (%)
$\alpha^2 = k_1 t$	56.6	19.0	3.49	17.1(35.1) ^a	10.0(17.7) ^a	5.92(6.01) ^a	13.9(34.2) ^a	6.6(19.2) ^a	6.27(6.94) ^a
$(1-\alpha)\ln(1-\alpha) + \alpha = k_2 t$	59.5	20.1	3.30	21.5(36.9)	13.7(18.7)	3.21(6.40)	16.9(37.6)	9.0(21.3)	3.69(8.40)
$[1-(1-\alpha)^{1/3}]^2 = k_3 t$	66.4	22.4	5.19	28.3(39.5)	18.7(19.5)	1.30(8.46)	22.2(43.5)	12.6(24.6)	0.83(8.17)
$1-(2\alpha/3)-(1-\alpha)^{2/3} = k_4 t$	61.3	19.6	1.43	23.7(37.7)	14.3(17.9)	0.76(2.93)	18.6(39.5)	9.1(21.3)	0.80(3.99)
$1-(1-\alpha)^{1/2} = k_5 t$	57.0	18.9	2.01	14.2(34.1)	7.3(16.7)	5.19(3.03)	13.6(33.0)	6.2(18.2)	5.26(3.42)
$1-(1-\alpha)^{1/3} = k_6 t$	59.0	19.6	1.24	16.2(35.0)	8.8(17.2)	3.53(2.28)	15.1(34.8)	7.2(19.1)	3.43(4.48)
$[-\ln(1-\alpha)]^{1/2} = k_7 t$	58.4	20.2	6.26	13.0(33.5)	6.8(17.1)	10.74(2.17)	14.0(32.5)	7.1(18.5)	10.40(7.51)
$[-\ln(1-\alpha)]^{1/3} = k_8 t$	56.3	18.9	6.43	10.4(32.2)	4.2(15.9)	9.09(4.67)	12.5(30.1)	5.4(16.5)	9.08(3.08)

^aThe value in parenthesis corresponds to the second reduction stage and st.dev. for the second stage of LaCoO_3 and $\text{LaNiO}_{2.92}$ is the value obtained at 467 °C and 439 °C, respectively.

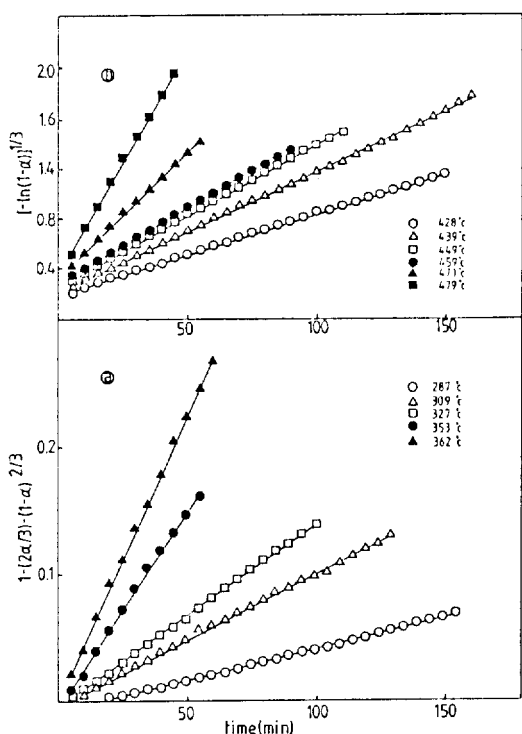


Figure 6. (a) Linear plots of $1-(2\alpha/3)-(1-\alpha)^{2/3}$ vs t for the first reduction stage of $\text{LaNiO}_{2.92}$. (b) Linear plots of $[-\ln(1-\alpha)]^{1/3}$ vs t for the second reduction stage of $\text{LaNiO}_{2.92}$.

is expressed as a term of contracting sphere mechanism (Table 3). This fact implies that rate controlling step on reduction of lanthanum iron oxide is chemical reaction²⁷ at reactant-product interface in contrast to above two mechanisms. Of course, this model is similar in rate process to diffusion model but it is distinct from the fact that overall rate process in the contracting sphere model is determined by the geometry of interface advance toward the bulk from the phase boundary.²⁵ However, it should be treated with care to conclude this fact because geometric interpretation must be supported by independent evidence, such as microscopic observations. The kinetic results confirmed in this work for the reduction of lanthanum iron oxide are contrast to the proposal by Tascon *et al.*¹³ who reported the nucleation mechanism. The present study, however, is well illustrated the reduction rate of lanthanum iron oxide as contracting

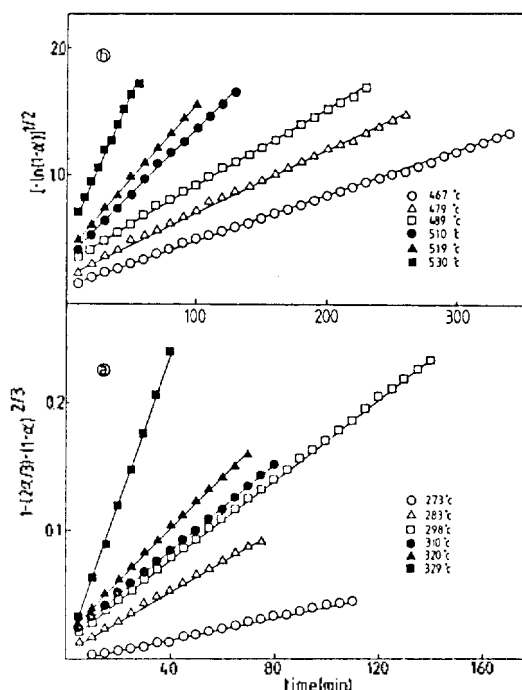


Figure 7. (a) Linear plots of $1-(2\alpha/3)-(1-\alpha)^{2/3}$ vs t for the first reduction stage of LaCoO_3 . (b) Linear plots of $[-\ln(1-\alpha)]^{1/2}$ vs t for the second reduction stage of LaCoO_3 .

sphere model (Table 3) not nucleation mechanism.

Figure 6, 7 and 5-b give the linear plots of appropriate reduction equation against time t . From the slopes, kinetic parameters (activation energy and preexponential term) are calculated as shown in Table 3. For the reduction of lanthanum nickel and cobalt oxides activation energies calculated by Ginstling-Brounshtein equation in the first stage are 18.6 and 237.7 Kcal mol⁻¹, and 30.1 and 33.5 Kcal mol⁻¹ of activation energy in the second stage are obtained by Avrami-Erofeev equation, respectively. And, activation energy of 59 Kcal mol⁻¹ is calculated from the contracting sphere model for the reduction of lanthanum iron oxide.

Conclusion

According to the results obtained by temperature-programmed reduction and isothermal reduction study, it is confirmed that oxygen stoichiometry of the sample perovskite

used in this work is $\text{LaFeO}_{3.18}$, $\text{LaCoO}_{3.06}$ and $\text{LaNiO}_{2.92}$, and that reducibility is in the following order: $\text{LaFeO}_{3.18} > \text{LaCoO}_{3.06} > \text{LaNiO}_{2.92}$. Lanthanum nickel and cobalt oxides are reduced *via* the formation of divalent ion (Ni^{2+} or Co^{2+}) as intermediate to 3-electron reduction while lanthanum iron oxide is directly reduced to 3-electron level. These results imply that the valence state of transition metal varied during reduction is an important factor to determine the physicochemical property of the perovskite. Reaction kinetics for the first and second reduction stages are followed by diffusion mechanism and nucleation mechanism, respectively, and reduction of lanthanum iron oxide is processed by contracting sphere mechanism. In addition, the value of activation energy on reduction of the perovskite is paralleled with the thermal stability. From this fact kinetic behaviors are also partly related in the reactivity of the perovskite.

Acknowledgement. The authors are grateful to the Seo Bong Culture Foundation, Seoul, for the financial support.

References

- W. F. Libby, *Science*, **171**, 499 (1971).
- R. J. H. Voorhoeve, J. P. Remeika, P. E. Freeland and B. T. Matthias, *Science*, **177**, 353 (1972).
- S. C. Sorenson, J. A. Wronkiewicz, L. B. Sis and G. P. Wirtz, *Am. Ceram. Soc. Bull.*, **53**, 446 (1974).
- D. W. Johnson, Jr., P. K. Gallagher, F. Schrey and W. W. Rhodes, *Am. Ceram. Soc. Bull.*, **55**, 520 (1976).
- S. George and B. Viswanathan, *Surf. Tech.*, **19**, 217 (1983); *J. Colloid and Inter. Sci.*, **95**, 322 (1983).
- J. M. D. Tascon, J. L. G. Fierro and L. G. Tejuca, *Z. Phys. Chem. (Neue Folge)*, **124**, 249 (1981).
- J. O. Petunchi, J. L. Nicastro and E. A. Lombardo, *J. Chem. Soc. Chem. Comm.*, 1980, 467.
- J. O. Petunchi, M. A. Ulla, J. A. Marcos and E. A. Lombardo, *J. Catal.*, **70**, 356 (1981).
- K. Ichimura, Y. Inoue and I. Yasumori, *Bull. Chem. Soc. Jpn.*, **53**, 3044 (1980); **54**, 1787 (1981).
- T. Arakawa, N. Ohara and J. Shiokawa, *Chem. Lett.*, 1984, 1467.
- M. Crespin, L. Gatineau, J. Fripiat, H. Nijs, J. Marcos and E. Lombardo, *Nouv. J. Chim.*, **7**, 477 (1983).
- T. Nitadori and M. Misono, *J. Catal.*, **93**, 459 (1985).
- J. M. D. Tascon, J. L. G. Fierro and L. G. Tejuca, *J. Chem. Soc., Faraday Trans. 1*, **81**, 2399 (1985).
- J. Mizusaki, T. Sasamoto, W. R. Cannon and H. K. Bowen, *J. Am. Ceram. Soc.*, **65**, 363 (1982); **66**, 247 (1983).
- R. J. H. Voorhoeve, J. P. Remeika and L. E. Trimble, *Ann. N. Y. Acad. Sci.*, **272**, 3 (1976).
- R. J. H. Voorhoeve, D. W. Johnson, Jr., J. P. Remeika and P. K. Gallagher, *Science*, **195**, 827 (1977).
- J. M. D. Tascon, S. Mendioroz and L. G. Tejuca, *Z. Phys. Chem. (Wiesbaden)*, **124**(1), 109 (1981).
- A. Word, B. Post and E. Banks, *J. Amer. Chem. Soc.*, **70**, 4911 (1957).
- S. H. Baek, M. S. Thesis, Sung Kyun Kwan University (1988).
- H. Taguchi, M. Shimada and M. Koizumi, *J. Solid State Chem.*, **29**, 221 (1979).
- G. H. Jonker and J. H. Van Santen, *Physica*, **19**, 120 (1953).
- I. H. Park and H. P. Lee, Private Communication.
- L. Wachowski, S. Zielinski and A. Burewicz, *Acta Chim. Acad. Sci. Hung.*, **106**, 217 (1981).
- T. Nakamura, G. Petzow and L. J. Gauckler, *Mat. Res. Bull.*, **14**, 649 (1979).
- D. Brennan, A. T. Fromhold, Jr., R. G. Fromhold, L. G. Harrison and Y. Koga, *Comprehensive Chemical Kinetics*, Vol. 21, Chap. 2, C. H. Bamford, C. F. H. Tipper and R. G. Compton, Eds., Elsevier, Amsterdam, The Netherlands, 1984.
- P. Anoldy, J. C. M. de Jonge and J. A. Moulijn, *J. Phys. Chem.*, **89**, 4517 (1985).
- N. W. Hrst, S. J. Gentry, A. Jones and B. D. McNicol, *Catal. Rev.-Sci. Eng.*, **24**, 233 (1982).
- B. Delmon and A. Roman, *J. Chem. Soc. Faraday Trans. 1*, **69**, 941 (1973).
- J. L. G. Fierro, J. M. D. Tascon and L. G. Tejuca, *J. Catal.*, **93**, 83 (1985).